Intracavity configuration for tuning and obtaining simultaneous dual-wavelength operation from CW Nd:YAG laser

Alireza Khorsandi* **and Saeed Ghavami Sabouri**

Department of Physics, Isfahan University, 81746-73441 Isfahan, I.R. Iran

**Corresponding author: a.khorsandi@phys.ui.ac.ir*

Received December 15, 2010; accepted February 21, 2011; posted online May 18, 2011

In this letter, a thin slab of glass is used as Fabry–Perot etalon inside a cavity of a continuous wave (CW) Nd:YAG laser to change the behavior of its output longitudinal modes. The slab etalon is used as tuning element when it turns around the laser cavity axis. Two simultaneous longitudinal modes with a relatively wide tuning range from 5.83 MHz to 0.02 THz are obtained when the Nd:YAG laser is operated at moderate output power of about 120 mW. The mode structure of this configuration is modeled and simulated. Computer-generated diagrams are also presented schematically and compared with the experimental results.

OCIS codes: 140.3460, 140.3600.
doi: 10.3788/COL201109.071404.

Nd:YAG crystal possesses ideal optical properties, including low threshold, ease of growth and thermoconductivity; it can also operate at room temperature[1]. The Nd:YAG laser is very efficient and is a relatively high-performance source for a wide range of applications in pure and applied physics[2]. Additional applications have been expanded to include machining of metals for industries as well as marking and repairing of semiconductor materials when the laser is equipped with fiber delivery systems[3,4]. In combination with nonlinear crystals, such as KTP and PPLN, Nd:YAG laser is capable of generating parametric radiations from visible to mid-infrared spectral region, where many molecular species exhibit strong absorption lines and the laser absorption spectroscopy is introduced as a very promising diagnostic technique[5–7]. Recently, optically pumped submillimeter wave generation devices, such as semiconductor antennas, have been developed, resulting in the dramatic increase of THz wave generation for security purposes[8,9].

In the case of THz generation either in semiconductor devices or through nonlinear optical crystals, a specific laser source possessing two closely longitudinal modes is essential. Different approaches have been proposed to develop tunable simultaneous dual-wavelength coherent sources since the first reported THz radiation in the last decade[10]. Of these, possibly the easiest method to achieve simultaneous dual-mode operation consists of the use of diode lasers provided in several schemes. Most of these approaches are also based on the process of using a tuning element, such as grating[11,12] or etalon[13] within a fabricated external cavity in the front part of a commercial diode laser. An external-short cavity in the front part of a simple diode laser can also be used to stabilize and control its spectral output[14]. Although the diode lasers are favorable in terms of low fabrication cost, single-mode operation and compactness, they suffer from low output power and sensitivity to electrical shocks. Nd:YAG lasers can operate with sufficient output power and under minimum environmental influences. The fluorescence spectrum of Nd:YAG exhibits several transitions in the $^4F_{3/2} \rightarrow {}^4I_{9/2}$, $^4I_{11/2}$, and $^4I_{13/2}$ manifolds that are suitable for many laser transitions[15]. An intracavity thin solid etalon, combined with a coated resonator mirror, has been used to tune its output wavelength over a comparable frequency range and hence obtaining additional lines[16]. Dual-longitudinal mode operation of the Nd:YAG laser has also been reported using two low-power seed lasers[17]. After adjusting the energy of each mode through the power of injected seed lasers, the obtained mode spacing ranged from 185 MHz to 17 GHz in increments of 185 MHz. Nearly at the same time, wide-bandwidth Ti:sapphire laser has also been chosen as an another candidate for dual-mode operation, in which a cavity based on Littman configuration and a partially reflecting feedback mirror are applied[18]. One example is given in this letter, in which a diode-pumped continuous wave (CW) Nd:YAG laser is shown to offer great potential for simultaneous dual-longitudinal mode operation. Low tuning range of the generated modes is still a limiting factor, and is determined by the narrow gain bandwidth of this high-performance solid-state laser.

In the 1970s, Marling used a thin, solid fused silica intracavity etalon in his experimental arrangement of a high-power Kr-arc pump Nd:YAG laser in order to excite 19 additional transitions beyond the fundamental 1,064-nm line[16]. By appropriate choice of the reflectivity of resonator mirrors as well as by adjusting the angle of uncoated intracavity etalons, he tuned each individual

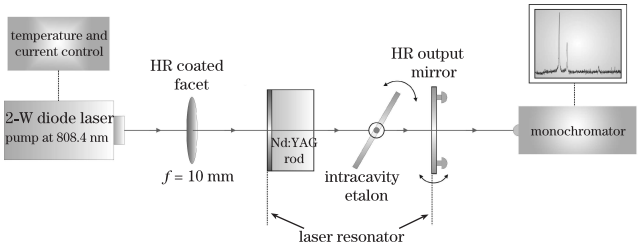

Fig. 1. Schematic diagram of intracavity experimental setup of a CW Nd:YAG laser for tuning and dual-mode operation.

line over a range of several wave numbers. Moreover, additional weak side bands and simultaneous dual-longitudinal modes can be generated in the spectral bandwidth of a Nd:YAG laser through the insertion of a glass plate into its cavity as tuning element.

An uncoated slab of glass used as Fabry–Perot (FP) etalon was used within the cavity of a CW Nd:YAG laser (Fig. 1). The investigated laser was provided commercially and used a high-power 2-W diode in a highly efficient end-pumped scheme. The laser rod was 5 mm in length and had a diameter of 5 mm. Its input facet was high-reflection (HR) coated to excite the strongest emission from Nd:YAG laser occurring at 1,064 nm. The coating was designed for maximum pump beam transition with about 85% output coupling. To minimize the cavity loss, the output facet of Nd:YAG road had a high-quality antireflection layer for 1,064 nm. The second resonator mirror was also coated for HR (about 99.95%) and mounted on a very precise three-dimensional translator to either permit lowest-order transverse mode, TEM_{00}, or maximize the spacing of the etalon rotating element around the optical axis of the resonator. An optimum resonator length of about 20 cm can be provided by this arrangement.

The necessary pumping wavelength and power for Nd:YAG lasing were attained by fixing the temperature and current of the 2-W diode laser pump at 28 °C and 2 A, respectively. The output beam of the pump source was then focused into the active medium using a high-quality imaging lens with a focal length of 10 mm. The Nd:YAG output power was kept nearly constant and stable at around 120 mW.

The intracavity etalon used in the experiment was a very thin slab of fused glass with submillimeter thickness of about 200 μm, which was fixed during the measurement. Its transmittance was $T \cong 30\%$. The intracavity insertion loss resulting from the components within the resonator was set on its minimum value. A convenient feature of this scheme is the ability to provide low lasing threshold of around 20 mW of the diode pump. The internal etalon was placed on a scaled rotating plate, enabling smooth tuning in a desirable range of angles with respect to the optical axis of the cavity.

As long as the facets of the internal etalon were kept parallel with the resonator mirrors, neither the side bands nor the mode tuning was observed. Under this condition only the fundamental lasing mode oscillating near

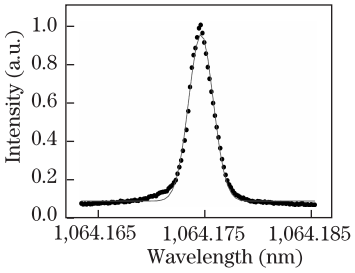

Fig. 2. Spectrum of the fundamental Nd:YAG laser oscillating within 1,064.1-nm band, while the internal etalon is not turned and keeps vertical. The laser bandwidth is $0.0023 \pm 2 \times 10^{-5}$ nm. Dots indicate recorded data throughout the calibrated monochrometer; the solid line indicates the fitted Gaussian profile.

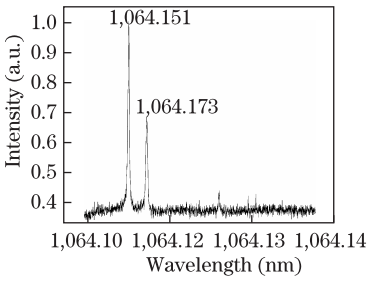

Fig. 3. Simultaneous dual-mode operation illustrating Nd:YAG laser tuning by angular variation of 200 μm intracavity etalon. The rotating angle θ is 35°. The FSR is measured at 0.022 nm, which is equal to 5.83 MHz.

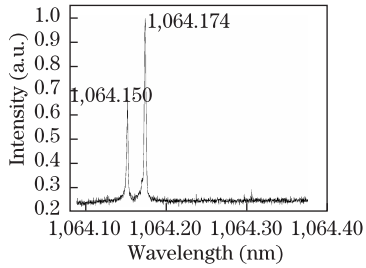

Fig. 4. Variations of the intensity of two modes with bigger etalon rotating angle, $\theta = 43°$ (compared with two picks shown in Fig. 3).

1,064 nm specified by the $^4F_{3/2} \rightarrow {}^4I_{11/2}$ transition became dominant. The spectrum of this fundamental laser mode was resolved by a grating-based monochrometer. The absolute calibration of the monochrometer was carefully performed using the well-known atomic transition lines of a standard discharged Argon lamp. The measured bandwidth of the recorded laser spectrum, $\Delta\lambda_{FWHM}$, is $0.0023 \pm 2 \times 10^{-5}$ nm (corresponding to about 0.6 MHz) by fitting the Gaussian profile into the experimental data, as shown in Fig. 2. If the intracavity etalon is turned with respect to the incident laser beam, the laser bandwidth can be further reduced due to the longer optical path inside the laser resonator. This setup without internal etalon provided wider laser bandwidth, which was in the order of a few megahertz. The presence of the etalon inside the laser resonator reduced the laser bandwidth to a few tenths of megahertz even if the etalon was not rotated. While the intracavity etalon is tuned, dual-mode operation is achieved. Figure 3 shows two longitudinal output modes while simultaneously oscillating with the measured free spectral range (FSR) of 0.022 nm. The pump diode was operated at a temperature and current of 28 °C and 2 A, respectively. The intensity ratio of the two modes is 1.45, which depends on the angle of the etalon. When the same condition for the pump diode is maintained at bigger etalon rotating angles the weaker line becomes stronger while spacing is slightly changed as shown in Fig. 4. The spacing of the two generated modes strongly depends on the rotating angle. When the tuning angle exceeded a certain angle, the spacing and intensity ratio of the two modes significantly changed, and lasing at a new wavelength became possible (Fig. 5). This remarkable variation was achieved by adjusting the rotating angle to $\theta = 70°$. At this rotating angle, mode spacing was 0.088 nm. This value is approximately equal to 23.3 MHz. The output

at 1,064.260 nm was approximately three times stronger than that of the output at 1,064.172 nm at the same pumping level. As a result, the insertion of a thin slab glass allowed the generation of simultaneous dual wavelengths.

According to Ref. [19]. the gain bandwidth of the Nd:YAG material in 1,064-nm band is in the order of few tenths of nanometers, which is quite larger than the etalon FSR specified in those three figures. The transmission maximum of two generated modes can be situated inside the gain envelop, through which simultaneous dual-mode operation becomes possible. The presence of etalon inside the laser resonator can lead to the bandwidth reduction of the laser spectrum. Similar behavior has also been reported in Ref. [20]. By turning the intracavity etalon inside the laser resonator, the optical path of the beam traveling in the cavity can then be increased. The consequence of the bigger turning angle is the provision of a longer optical path which, in turn, leads to the reduction of the laser bandwidth. This is because the laser bandwidth is inversely proportional to the optical path length of the traveling beam. For comparison, the bandwidth of the laser line labeled as 1,064.260 nm in Fig. 5 is measured and depicted in Fig. 6. As is measured, the laser bandwidth is slightly reduced and is about 3×10^{-4} nm less than the bandwidth of the fundamental Nd:YAG laser mode shown in Fig. 2.

A mathematical model describing the dynamic emission of intracavity Nd:YAG laser is adopted in the following. In many related textbooks, mode selection procedures in different kinds of lasers using intracavity etalon have been discussed[21]. There are two main multiple FP systems. The first is the combination of FPs in series, and the second consists of one FP within the cavity of another FP to form an intracavity configuration. This

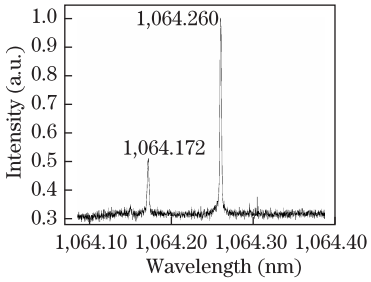

Fig. 5. Remarkable variation of both spacing and intensity of two generated modes while the pump diode was fixed at the same condition as 28 °C and 2 A.

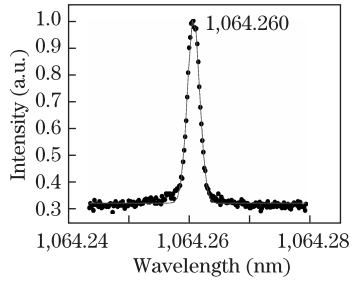

Fig. 6. Spectrum of the laser line labelled as 1,064.260 nm in Fig. 5. Dots indicate recorded data throughout the calibrated monochrometer; the solid line indicates the fitted Gaussian profile.

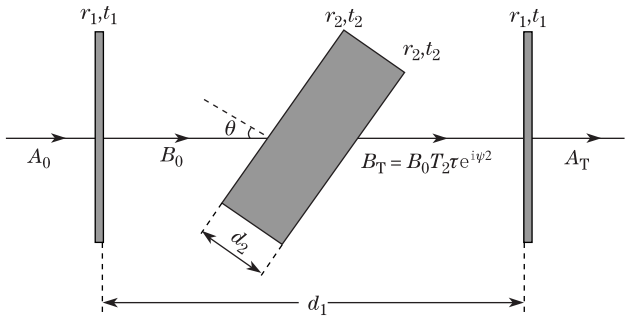

Fig. 7. Tilted etalon as a tuning element inside a laser and $r_1 r_2$ are the reflection coefficients, and t_1 and t_2 are the transmission coefficients.

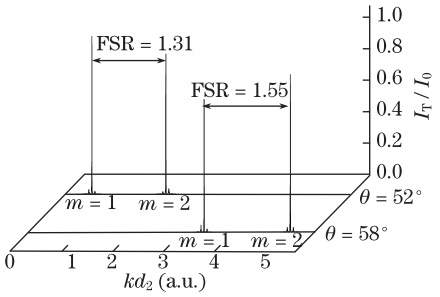

Fig. 8. Transmitted intensity of the intracavity scheme for two different etalon rotating angles for $d_1 = 15d_2$, $R_1 = 90\%$, and $R_2 = 65\%$. m is the interference order.

letter focuses on the latter. Based on the Schawlow–Townes limitation, the bandwidth of the laser emission is determined by the resonator characteristics; therefore, the effect of the gain medium is not considered in our investigation. The Nd:YAG gain bandwidth is wide enough to amplify the intracavity etalon transmission maxima as measured and extracted from the experimental results.

The transmission function of an intracavity laser system can be modeled analytically by starting with the assumption that the absorption of laser light on the surfaces is negligible. Basically, the emerging beam of λ from a typical FP interferometer with mirror spacing of d is characterized by either phase shift φ or amplitude variation. Those effects can be summarized in the following relation:

$$A_T = T\tau\ A_0\ e^{i\psi}, \tag{1}$$

with

$$\psi = \tan^{-1}\left(\frac{R\sin\varphi}{1 - R\cos\varphi}\right),$$

$$\tau = \frac{1}{\sqrt{(1 - R\cos\varphi)^2 + R^2\sin^2\varphi}},$$

and

$$\varphi = \frac{4\pi}{\lambda} d\cos\theta, \tag{2}$$

where A_T is the amplitude of emerging beam; τ is the amplitude coefficient; R and T are the reflectance and transmittance of the cavity mirrors, respectively; and θ is the angle of incident beam. Equation (1) can be extended for an FP including an internal etalon. To follow that, the intracavity configuration is assumed to be the same as that depicted in Fig. 7.

For the inner etalon, the field amplitude transmission coefficient $B_T = B_0 T_2 \tau\ e^{i\psi_2}$, can be obtained from

Eq. (2) for R_2, d_2 given by

$$\varphi_2 = \frac{4\pi}{\lambda} d_2 \cos\theta. \quad (3)$$

The total transmitted amplitude of the laser beam A_{T} coming out of the whole intracavity configuration, which is constituted by successive transmitted rays, can then be written as

$$A_T = A_0 T_1 T_2 \tau e^{i\psi_2}\{1 + T_2^2 R_1 \tau^2 e^{i(\varphi_1+2\psi_2)} + [T_2^2 R_1 \tau^2 e^{i(\varphi_1+2\psi_2)}]^2 + [T_2^2 R_1 \tau^2 e^{i(\varphi_1+2\psi_2)}]^3 + \cdots\}. \quad (4)$$

Therefore, the correspondence relative intensity of the above transmitted wave is given by

$$\frac{I_{\mathrm{T}}}{I_0} = \frac{(T_1 T_2 \tau)^2}{(1 - T_2^2 R_1 \tau^2)} \times \frac{1}{1 + F\sin^2(\frac{\varphi_1}{2} + \psi_2)}, \quad (5)$$

where

$$F = \frac{4 T_2^2 R_1 \tau^2}{(1 - T_2^2 R_1 \tau^2)^2}. \quad (6)$$

Figure 8 is the plot of Eq. (4) showing the capability of intracavity configuration providing very narrow bandwidth and broad FSR for the laser emission at λ = 1,064 nm when the intracavity etalon is adjusted for different values of intracavity spacing d_2, and its rotating angles θ. Wider FSR is also possible when the inner etalon is tilted over a certain angle as shown in Fig. 8. This configuration can be operated as an interferometric filter to omit the undesirable laser modes and tune the output beam on specific longitudinal ones. Once the etalon spacing is determined, its tilting angle can be tuned over a desirable range, making simultaneous dual-mode operation possible. One physical explanation is the simultaneous formation of two different cavity lengths inside the laser resonator. The model presented above can be extended to derive a transmitted intensity function of this structure by summation of the expression given in Eq. (5) over the intensity of individual modes. The result of this physical interpretation is shown in Fig. 9, which shows that our physical interpretation confirms the experimental observations specified in Figs. 3–5. The spacing of two modes is also increased due to bigger rotating angles of internal etalon.

In conclusion, we show that the result of using intracavity configuration to modify the mode behavior of a Nd:YAG laser is quite significant. This configuration enables the simultaneous generation of dual-longitudinal modes. Compared with other tunable dual-mode laser devices, the present apparatus can be evaluated as solid-state high-power source providing moderate tunability from about a few tenths to several terahertz. Those two closely generated modes can be used in nonlinear devices, such as difference-frequency schemes, as they are mixed through interaction with high-optical-quality nonlinear crystals, such as DAST. The mode spacing has been observed to be slightly sensitive to the rotating angle of the internal etalon. This tunability with the variable thickness of the internal etalon is worth checking. With the full analysis of an FP intracavity etalon, a mathematical description for the dynamic emission of the present configuration has been modeled and discussed in this letter. This simple technique can be extended to other wide-bandwidth solid-state laser materials, such as Yb:YAG and Nd:YVO_4 composites.

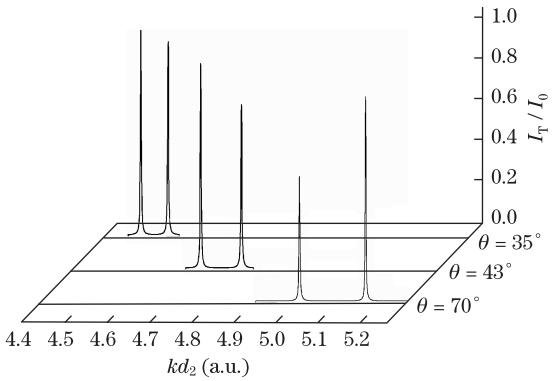

Fig. 9. Computer-generated graph of the transmitted intensity function for simultaneous dual-mode operation produced by intracavity configuration. This simulation is performed for d_1 = 18 d_2, R_1 = 90%, and R_2 = 75% close to the experimental values.

References

1. D. Sangla, F. Balembois, and P. Georges, Opt. Express **17,** 10091 (2009).
2. C. Bauer, P. Geiser, J. Burgmeier, G. Holl, and W. Schade, App. Phys. B **85,** 251 (2006).
3. D. P. Hand and J. D. C. Jones, Appl. Opt. **37,** 1602 (1998).
4. H. Jelinkova, J. Sulc, P. Cerny, Y.-W. Shi, Y. Matsuura, and M. Miyagi, Opt. lett. **24,** 957 (1999).
5. M. R. McCurdy, Y. Bakhirkin, G. Wysocki, R. Lewicki, and F. K. Tittel, J. Breath Res. **1,** 014001 (2007).
6. C. Bohling, D. Scheel, K. Hohmann, W. Schade, M. Reuter, and G. Holl, Appl. Opt. **45,** 3817 (2006).
7. A. Ngai, S. Persijn, G. Von Basum, and F. Harren, App. Phys. B **85,** 173 (2006).
8. D. Dragoman and M. Dragoman, Prog. Quantum Electron. **28,** 1 (2004).
9. T. Taniuchi, S. Ikeda, S. Okada, and H. Nakanishi, Jpn. J. Appl. Phys. **44,** L652 (2005).
10. D. M. Mittelmann, R. H. Jacobsen, and M. C. Nuss, IEEE J. Sel. Top. Quantum Electron. **2,** 679 (1996).
11. J. F. Lepage and N. McCarthy, Appl. Opt. **37,** 8420 (1998).
12. V. Zambon, M. Piche, and N. McCarthy, Opt. Commun. **264,** 180 (2006).
13. G. Baili, L. Morvan, M. Alouini, D. Dolfi, F. Bretenaker, I. Sagnes, and A. Garnache, Opt. Lett. **34,** 3421 (2009).
14. A. Khorsandi, U. Willer, P. Geiser, and W. Schade, App. Phys. B **77,** 509 (2003).
15. P.-X. Li, D.-H. Li, C.-Y. Li, and Z.-G. Zhang, Chin. Phys. **13,** 1689 (2004).
16. J. Marling, IEEE J. Quantum Electron. **QE-14,** 56 (1978).
17. T. Raymond and A. Smith, IEEE J. Quantum Electron. **31,** 1734 (1995).
18. D. K. Ko, G. Lim, S. H. Kim, B. H. Cha, and J. Lee, Opt. Lett. **20,** 710 (1995).
19. W. Koechner, *Solid-State Laser Engineering* (6th rev. and updated ed.) (Springer, New York, 2006).
20. M. Luhrmann, C. Theobald, R. Wallenstein, and J. A. L'huillier, Opt. Express **17,** 6177 (2009).
21. C. Ye, *Tunable External Cavity Diode Lasers* (World Scientific, Hackensack, 2004).